Experience shapes the transformation of olfactory representations along the cortico-hippocampal pathway

Eleonore Schiltz[1], Martijn Broux[1], Cagatay Aydin[1,2,5], Pedro Goncalves[1,3,4], Sebastian Haesler[1,2]

[1]Neuroelectronics Research Flanders (NERF), Leuven, Belgium
[2]Department of Neurosciences, KU Leuven, Leuven, Belgium
[3]Department of Computer Science, KU Leuven, Leuven, Belgium
[4]Department of Electrical Engineering, KU Leuven, Leuven, Belgium
[5]Department of Biomedical Engineering, Bahcesehir University, Istanbul, Turkey.
*Correspondence: sebastian.haesler@nerf.be

ABSTRACT

Perception relies on the neural representation of sensory stimuli. Primary sensory cortical representations have been extensively studied, but how sensory information propagates to memory-related multisensory areas has not been well described. We studied this question in the olfactory cortico-hippocampal pathway in mice. We recorded single units in the anterior olfactory nucleus (AON), the anterior piriform cortex (aPCx), lateral entorhinal cortex (LEC), the hippocampal CA1 subfield, and the subiculum (SUB) while animals performed a non-associative learning paradigm involving novel and familiar stimuli. Novel stimuli evoked larger responses than familiar stimuli in the AON, whereas in hippocampal areas, novelty was reflected by the number of responsive neurons. In parallel, odorant selectivity increased along the pathway. While both stimulus identity and experience were thus reflected in all regions, their neural representations gradually separated. Our findings provide a potential mechanism for how sensory representations are transformed to support stimulus identification and implicit memories.

KEYWORDS

sensory system, hippocampus, olfactory cortex, non-associative learning, memory, novelty, experience

INTRODUCTION

Sensory systems form a neural representation of the outside world inside the brain by converting physical stimuli into sequences of action potentials. These neural representations enable the detection, identification, and discrimination of stimuli in the environment. The representation of stimuli in primary auditory, visual, somatosensory, and olfactory cortices has been studied extensively (deCharms and Zador, 2000; Kriegeskorte and Wei, 2021), but how stimulus representations transform from primary sensory to multisensory areas is not well described. Moreover, cortical representations are not static, but they undergo changes over shorter (>seconds; Homann et al., 2022; Ulanovsky et al., 2003) and longer (>days; Frenkel et al., 2006; Schoonover et al., 2021; Woloszyn and Sheinberg, 2012) timescales. Nonetheless, non-instrumental stimuli can be remembered in large number (Standing, 1973) and with remarkable detail (Brady et al., 2008). While non-associative learning can thus create vast, implicit memory of stimuli in the environment, it is unclear how stimulus representations reflect this memory.

Here, we characterized the transformation of neural representations from cortical primary sensory to multisensory areas in the medial temporal lobe and investigated how they were affected by non-associative learning. We focused on the olfactory system, which contrary to visual, auditory, and somatosensory systems lacks thalamo-cortical pathways. Mitral and tufted cells, the output neurons of the olfactory bulb (OB), directly project to primary olfactory cortical areas, including the anterior olfactory nucleus (AON) and the anterior piriform cortex (aPCx) through the lateral olfactory tract (LOT) fiber bundle (Brunjes et al., 2005; Cleland and Linster, 2019). The LOT further provides input to the lateral entorhinal cortex (LEC), a multisensory structure (Tsao et al., 2013; Wu et al., 2023) situated at the intersection with the hippocampal region. The LEC, in turn, projects to the hippocampal CA1 subfield and the subiculum (SUB), a major output of the hippocampal formation (Witter et al., 2000). This olfactory cortico-hippocampal pathway is further characterized by extensive feedforward and feedback connections between the AON, aPCx, and LEC (Haberly and Price, 1978; Leitner et al., 2016; Neville and Haberly, 2003; Su et al., 2009, p. 209) on one hand and the LEC, CA1, and SUB on the other (Craig and Commins, 2007; Witter and Moser, 2006).

Non-associative learning modulates olfactory neural representations already in the OB, the first processing stage of the olfactory pathway. Brief, repeated odor experience leads to a gradual and long-lasting weakening of mitral cell odor representations in awake mice (Kato et al., 2012). In the aPCx, which has been suggested as a site of perceptual learning (Wilson and Stevenson, 2003), repeated presentation of odorants leads to short-term habituation (Wilson, 1998). Over longer time scales, neurons have been observed to lose their responsiveness to odors unless they are frequently exposed to them, which has been interpreted as representational drift (Schoonover et al., 2021). How non-associative learning affects olfactory representations in the other structures of the olfactory hippocampal pathway, namely the AON, the LEC, CA1, and SUB, has not been reported.

To investigate the transformation of odorant representations across multiple brain areas along the cortico-hippocampal pathway, we used high-density neural probes (Steinmetz et al., 2021; Van Daal et al., 2021) to record more than 1400 neurons in the AON, aPCx, LEC, (ventral) CA1, and SUB of mice performing an olfactory non-associative learning paradigm, in which we presented familiar and novel odors. This paradigm allowed us to compare the encoding of chemical identity between regions and analyze at the cellular and population level how representations are shaped by experience.

RESULTS

Olfactory responses in the cortico-hippocampal pathway

We used a non-associative olfactory learning paradigm (Rabell et al., 2017) in which we repeatedly presented four odorants in random order to head-restrained mice (n = 16) in one daily session over four consecutive days (long-term habituation, Figure 1A). After this familiarization period, we recorded single units along the olfactory pathway (Figure 1B), specifically in the AON (n = 215), aPCx (n = 266), LEC (n = 233), CA1 (n = 474) and SUB (n = 186). We identified significant odor responses by comparing the firing rate before and after the onset of the odor with a Wilcoxon rank test (Bolding et al., 2020). In all areas investigated, we found odorant-responsive neurons (Figures 1C and 1D). The fraction of neurons that responded significantly to at least one odor was slightly larger in the AON and aPCx than in the LEC, CA1, and SUB, but overall differences were not significant (Figure 1E).

In other sensory modalities, it has been observed that neuronal spike train statistics are different between primary sensory and multisensory neocortex. The interspike-intervals (ISI) of neurons in sensory areas follow Poisson-like statistics, whereas multisensory regions tend to exhibit more regular firing (Maimon and Assad, 2009; Shin and Moore, 2019). Fitting a gamma function to the ISI distributions of each recorded brain area reveals a similar pattern for the olfactory hippocampal pathway. Only for AON and aPCx, the shape or alpha parameters of the fitted gamma functions were close to 1, indicating a Poisson-like spiking dynamic (Figures 1F and 1G). The LEC, CA1, and SUB showed larger alpha values, consistent with more regular firing. While responses to odorants are thus found throughout the pathway, only AON and aPCx exhibit characteristics observed in sensory neocortex.

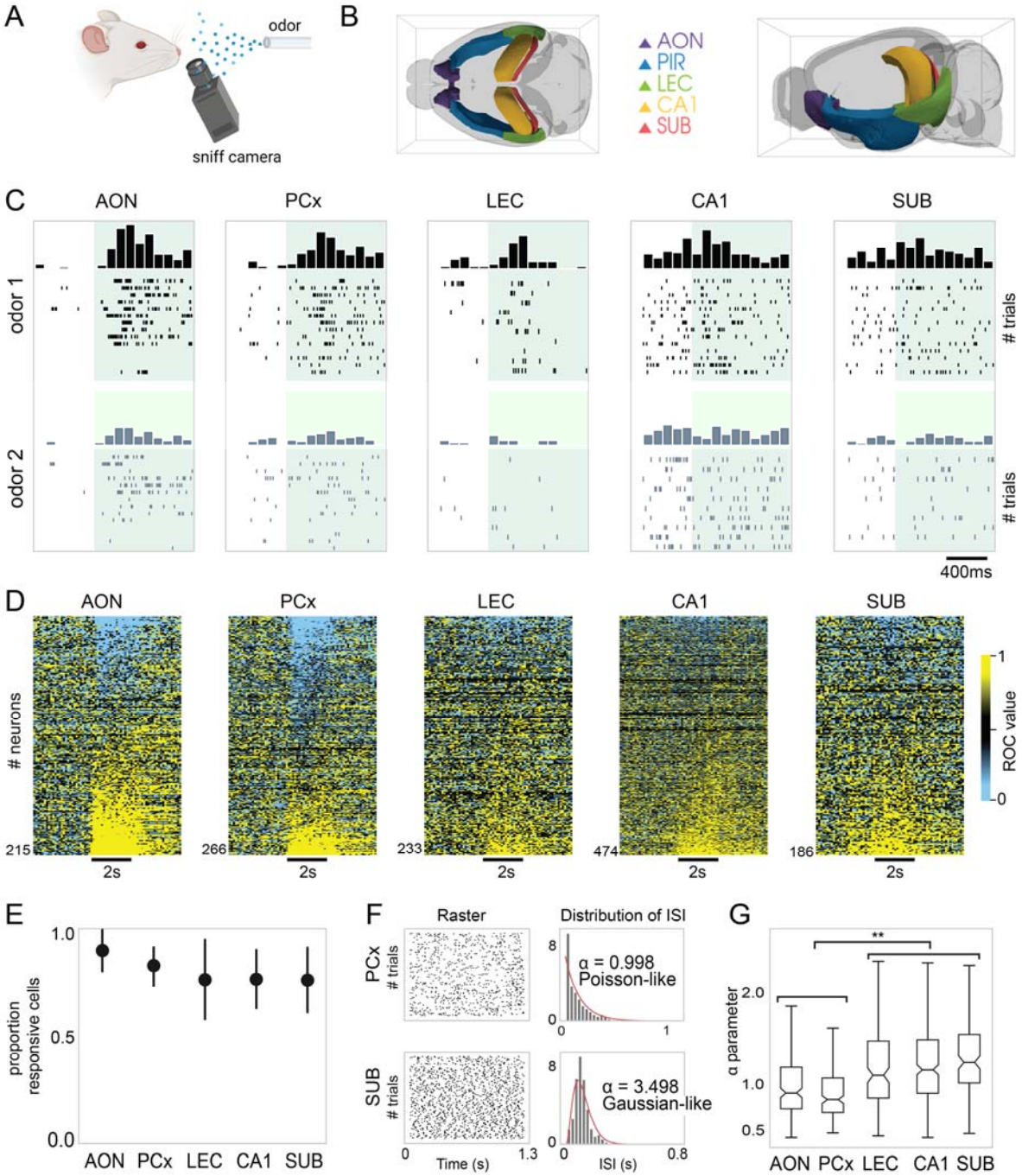

Figure 1. Olfactory responses in the cortico-hippocampal pathway. (A) Schematic representation of the experimental setup. Infrared thermography was used to measure respiration. **(B)** Illustration of recorded brain areas AON, aPCx, LEC, CA1, and SUB. **(C)** Example of neurons responding to either of two different familiar odors in each of the five recorded areas. Green shading indicates the time window of odor delivery. **(D)** Responses of all recorded neurons (n=1414) to familiar odors. Yellow indicates an increase from baseline, blue indicates a decrease. Each row represents one neuron. **(E)** Fraction of recorded neurons per area responding to at least one odor. Odor responsiveness per area (not significant, $p>0.3$, Kruskal Wallis test). Error bars: ± standard deviation (SD) between experiments. **(F)** Raster plot during presentation of odors for two example neurons in the aPCx (top) and the SUB (bottom). Histogram of the ISI for those neurons and fitting value of gamma function (right). **(G)** Distribution of alpha parameters ($p<0.01$, Kruskal-Wallis). AON and aPCx significantly different from LEC, CA1, and SUB ($^{**}p<0.01$, Mann-Whitney).

Experience modulates odor responses across the cortico-hippocampal pathway

To investigate the impact of non-associative learning on odorant representations along the olfactory hippocampal pathway, we introduced novel stimuli randomly interleaved with familiar stimuli in our olfactory paradigm. This paradigm allowed us to directly compare how chemical identity and experience (i.e., stimulus familiarity) are represented in different brain areas.

It is well established that novel odorants evoke a stereotypical increase in respiration frequency, also referred to as exploratory sniffing (Wesson et al., 2008). We used exploratory sniffing as a behavioral measure of experience. As expected, mice responded to novel stimuli with a significant increase in breathing rate (Figure S1A, $p<0.01$, paired t-test). Within one experimental session, behavioral responses to novel stimuli habituated with recurrent stimulus presentation (short-term habituation, Figure S1A) such that they became indistinguishable from those to long-term habituated, familiar stimuli ($p>$ 0.1, paired t-test, after three stimulus presentations).

Experience affected neuronal odorant responses in all regions studied (Figure 2A). The differential behavioral response to novel and familiar stimuli might confound the analysis of the effect of experience on sensory representations, in particular in regions in which respiration modulates spiking activity (Bathellier et al., 2008; Bolding and Franks, 2018). Therefore, we focused all further analysis on a 400ms window around the first inhalation after odor onset, when the respiration rate was not yet diverging between novel and familiar stimuli (Figures 2B and S1B). In this time window, novel stimuli evoked larger responses than familiar stimuli, in particular in the AON. The impact of novelty on response magnitude gradually decreased towards the posterior regions (Figure 2C).

Next, we compared the odor selectivity of neurons between regions. We determined how selectively neurons encoded different chemicals by counting the number of stimuli each neuron significantly responded to. We found marked differences between primary sensory and multisensory regions (Figure 2D). Stimulus selectivity was lowest in the AON (mean=4.1±1.5 SD) and gradually increased from aPCx (3.0±1.0) to LEC (2.3±0.7), CA1 (2.4±0.8), and SUB (2.3±0.8).

We then asked how selectively neurons encoded novelty and familiarity. We determined for each neuron whether it significantly responded to odorants of the novel, the familiar or both stimulus categories (Figure 2E). In primary sensory regions, both novel and familiar stimuli activated a large fraction of neurons, suggesting a mixed representation of chemical identity and experience. In the LEC, CA1, and SUB, on the other hand, a large fraction of neurons was selective just for novel stimuli.

To characterize sensory representations at the population-level, we used a linear Support Vector Machine (SVM). First, we focused on the representation of stimulus identity and decoded the chemical identity of odorants from neuronal firing rates during the analysis window across all experimental sessions (Figures 2F and 2H). The decoding accuracy was above chance level in all areas, indicating that the information about odorant identity is preserved throughout the pathway. The highest accuracy values were obtained in the AON, all other structures showed a marked decrease in decoding accuracy for odor identities in the population.

Next, we analyzed the encoding of experience in the neuronal population from each region by training a SVM to classify novel vs. familiar trials. Since we had found earlier that odor identities could be decoded from the neural data, the SVM might recover the information about experience solely based on odor identity. To address this potential confound, we compared the decoding accuracy of novel versus familiar odors with the decoding accuracy of two groups of randomly selected odors ("*shuffled*").

The decoding accuracy was higher for experience than for the shuffled odors, indicating that neurons reflected odorant experience. We found the highest decoding accuracy of experience in the AON, while all other regions showed similar, lower levels of accuracy (Figure 2G and 2I). The neural representation in the AON thus showed the highest decoding accuracy for both odor identity and experience.

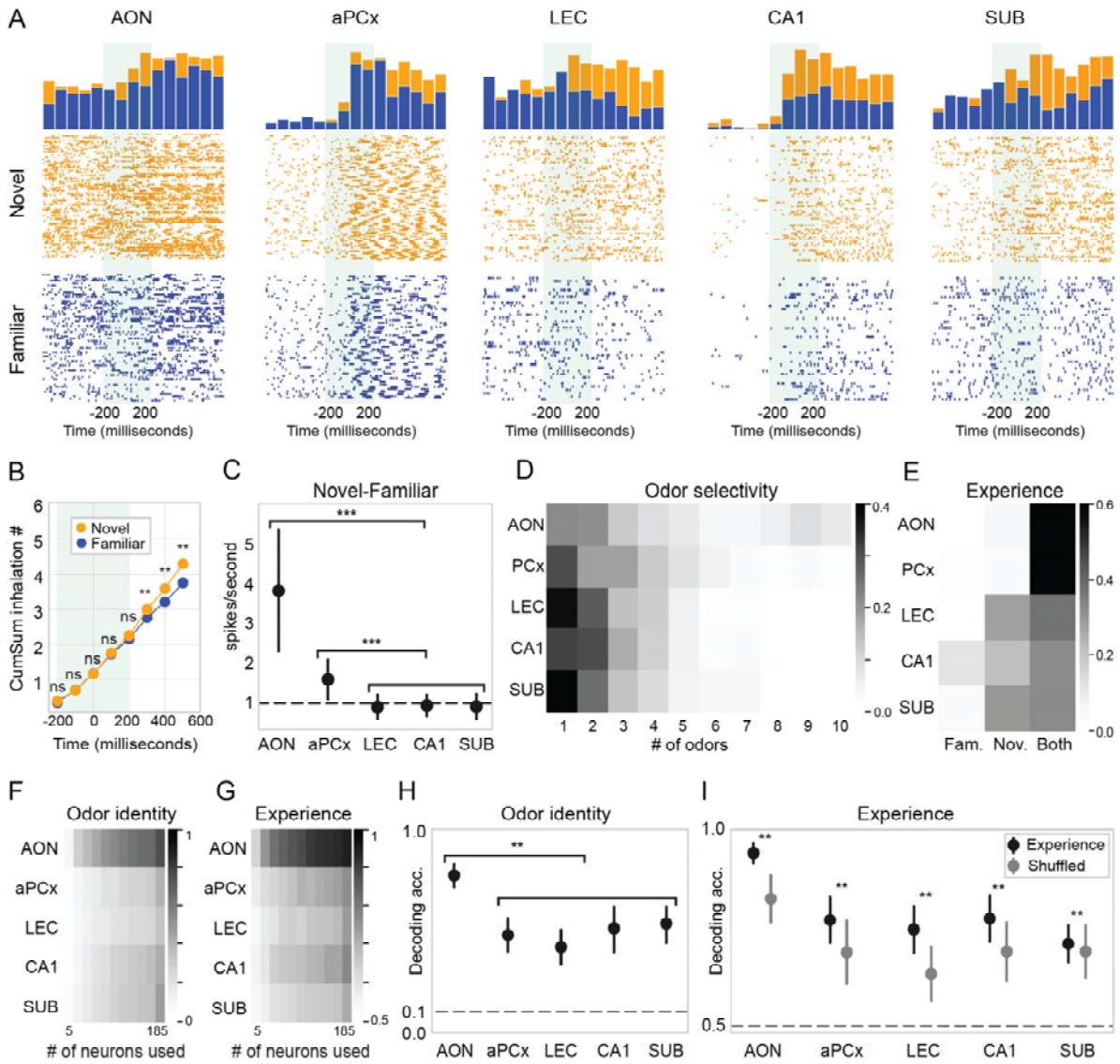

Figure 2. Experience modulates odor responses across the cortico-hippocampal pathway. (A) Example raster plots of two neurons in each brain area during the presentation of familiar and novel odors. The analysis window is highlighted in green in the raster plots. **(B)** Cumulative inhalation counts for all experiments in the time window around odorant delivery (time point 0). All subsequent analyses were performed in a 400ms analysis window (highlighted in green), when breathing was indifferent between novel and familiar conditions (*ns*: not significant, $^{*}p<0.05$, $^{**}p<0.01$, paired t-test). **(C)** Absolute difference in firing rate between the average response to novel and familiar odors per neuron. ($p<0.001$, Kruskal Wallis). AON and aPCx significantly different from every other region ($^{***}p<0.001$, Mann-Whitney). Error bars: 95% CI of the mean. **(D)** Fraction of neurons with significant responses to a given number of odorants (1-10). **(E)** Fraction of neurons with significant responses to odors of either familiar, novel, or both stimulus categories. **(F)** Decoding accuracy of odor identities calculated for an increasing sample of neurons. **(G)** Decoding accuracy of experience calculated for an increasing sample of neurons. To ensure accuracy can be compared between regions, we subsampled in each region the largest common number of neurons recorded (185 neurons). **(H)** Decoding accuracy of odor identities ($p<0.01$, ANOVA). The AON significantly differed from all other regions ($^{**}p<0.01$, Student's t-test). Error bars: 95% CI of the mean. **(I)** The decoding accuracy of experience (black, *Experience*) was significantly higher than the decoding accuracy of randomly associated odorants (grey, *Shuffled*) in all regions ($^{**}p<0.01$, paired t-test). The decoding accuracy was also significantly different between regions ($p<0.01$, ANOVA). The AON had a significantly larger decoding accuracy than any other region ($p<0.01$, Welch t-test). Error bars: SD.

A small subpopulation of neurons in the aPCx is tuned to familiar stimuli.

Non-associative learning creates implicit memories of stimuli in the environment. To investigate how this memory is reflected in the sensory representations, we compared the encoding of odor identities between

novel and familiar conditions. Using an SVM to decode odorant identity separately for novel and familiar odorants, we found that experience impacts the representation of stimulus identity (Figure 3). Specifically, the aPCx showed much higher decoding accuracy for familiar odors than novel ones (Figure 3A). This might suggest the population of aPCx neurons is particularly tuned to familiar odorants. To investigate this further, we calculated the mutual information between neuronal firing and odorant identity, separately for novel and familiar conditions (Figure 3B). This measure indicates how much knowing the firing rates reduces the uncertainty about the identity of odorants. Surprisingly, mutual information was similar for novel and familiar conditions in the aPCx indicating no specific tuning of the whole population to familiar odorants. But how could the SVM then have achieved a much higher accuracy in decoding the identity of familiar odorants compared to novel ones (Figure 3A) ?

During the training of the linear SVM, each neuron receives a weight that determines its relative contribution to the classification decision (Figure 3C). Importantly, a relatively small number of neurons with a large weight can have a decisive impact on classifier performance, yet they might not affect measures such as mutual information. When examining the weight distributions of SVMs for encoding familiar and novel odor identity, we found that the weights for decoding familiar odorants in the aPCx had a long tail of outliers (Figure 3D). We calculated the mutual information for outlier subpopulations across all brain areas, corresponding to an average of 5.2% (± 0.8 SD) of the data for each brain area (Figure 3E). The mutual information of the outlier population now captured the differences in the accuracy of encoding familiar and novel odorants observed in the SVM (Figure 3A), in particular in the aPCx but also the LEC and CA1 regions.

Collectively, these results indicate the presence of a subpopulation of neurons in the aPCx that are particularly tuned to odorants when they are familiar, as well as a subpopulation of neurons in the LEC and CA1 tuned to novel odorants. This analysis highlights that long-term, non-associative learning can refine the tuning of small fractions of neurons.

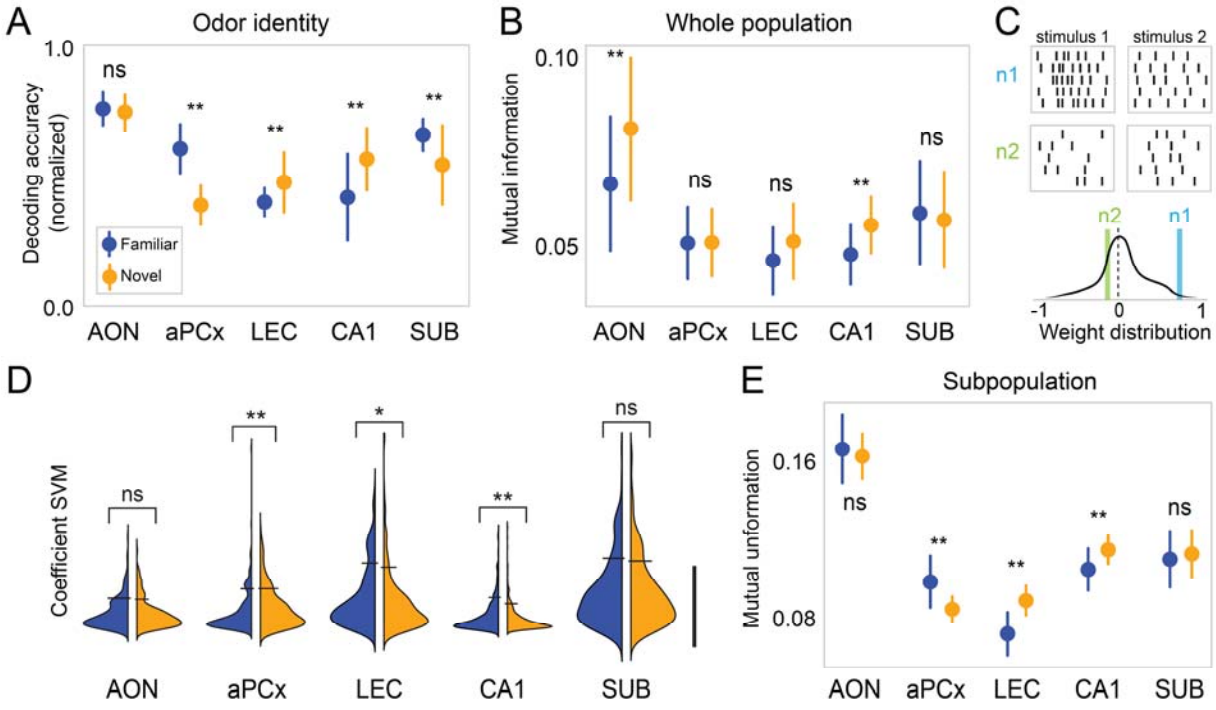

Figure 3. A subpopulation of neurons in the aPCx is tuned to familiar stimuli. (A) Accuracy of decoding the chemical identity of familiar and novel odors ($^{*}p<0.05$, $^{**}p<0.01$, paired t-test). Error bars: 95% CI of the mean. **(B)** Mutual information (MI) between odor identities and neuronal responses ($^{**}p<0.01$, paired t-test). Error bars: 95% CI of the mean. **(C)** Top: Simplified classification scheme in which two neurons contribute differently to decoding stimulus identity. The weight vector is orthogonal to the hyperplane separating the data. Bottom: Distribution of weights of all neurons. Neuron 1 (n1, blue) has a large weight, neuron 2 (n2, green) has a low weight in encoding stimulus identity. **(D)** Distribution of weights (absolute values) of the SVMs decoding the identity of either novel or familiar odorants.

Significant differences were observed in aPCx, CA1, and LEC (*ns*: not significant, $^{*}p<0.05$, $^{**}p<0.01$, Wilcoxon rank-sum test). **(E)** MI of outlier subpopulations (*ns*: not significant, $^{**}p<0.01$, Welch's t-test). Error bars: 95% CI of the mean.

The representations of odor identity and experience become independent from each other along the cortico-hippocampal pathway.

The presence of neuronal subpopulations specifically tuned to familiar odors in aPCx and to novel odors in LEC and CA1 (Figures 3A and 3E) raises the general question of how much each neuron contributes to encoding individual stimulus features. Do separate groups of neurons represent different stimulus features, or do all neurons form a continuous distribution for "multiplexed" encoding of odorant identity and experience?

To address this question, we analyzed the weights of the SVM trained to classify odorant identity. We did this separately for novel and familiar odors. If the same neurons which were good at classifying the chemical identity of the familiar odors were also good at identifying the chemical identity of the novel odors, their weights should be correlated. We found that SVM weights were increasingly correlated across the olfactory pathway from AON to SUB (Figure 4A). This suggests that neurons specialized in encoding chemical identity, independent of experience.

If this was indeed the case, it should also be reflected in the errors made by the SVM. If a neuronal population is specialized in encoding chemical identity irrespective of experience, a classification error will correspond to mistaking an odor for any other odor. On the other hand, if separate populations encoded familiar and novel odors, a SVM should mostly mistake familiar odors for other familiar odors and novel odors for other novel odors (Figure 4B). Analyzing the SVM errors for each brain area, we found a shift from making errors within the same category (i.e., the decoder mistakes a familiar odor for another familiar odor or a novel odor for another novel odor) to mistakes being made interchangeably between novel and familiar categories (Figure 4C).

The finding that encoding stimulus identity becomes independent of experience in multisensory areas is further supported by analysis of neuronal firing at the population level. We used principal component analysis (PCA) to investigate the position of novel and familiar trials in neural space. Notably, the representations of stimulus identity were separated between novel and familiar stimuli in AON and aPCx, while they became increasingly similar in multisensory areas (Figure 4D).

To quantify this effect, we calculated the Euclidean distance between novel and familiar trials on the one hand and between all trials irrespective of experience on the other. In AON, aPCx and LEC, the distance between novel and familiar trials was significantly higher than when not taking experience into account. Conversely, in the SUB, novel and familiar trials were significantly closer than the average distance between all trials (Figure S2A). The ratio of the two Euclidean distance measures revealed a significant, progressive decrease in distance between familiar and novel trials along the pathway (Figure 4E).

Given the representation of odorant identity gradually became independent from the representation of experience, we then asked if there was a distinct population of neurons encoding experience, independent of odorant identity. The SVM could decode experience in the multisensory areas with high accuracy (Figure 2I), but we found little evidence for the emergence of neurons that specifically responded in a stimulus-invariant manner to all novel or all familiar stimuli (novel 1/1414s and familiar 2/1414; Grubbs test confirmed stimulus-invariant neurons were not rare outliers of the distribution; see methods). Instead, we observed an increasing odor selectivity in multisensory areas (Figure 2D) and the emergence of a population of neurons responding significantly to specific odors only when they were novel (Figure 2E). Across the olfactory-hippocampal pathway, if a neuron responded to at least one novel odor, it had a decreasing probability of also responding to a familiar odor (Figure 4F). These observations imply that the number of odor-responsive neurons reflects experience. In any given trial, the more neurons were activated by a stimulus, the more likely the stimulus was novel.

In conclusion, we found a gradual transformation of sensory representations from primary sensory to multisensory areas, during which the representations of odorant identity and experience became increasingly independent from each other. This gradual transformation of sensory representations coincided with

increasing response reliability, as we observed that the variance of neuronal responses progressively decreased from AON to medial temporal lobe structures (Figure 4G).

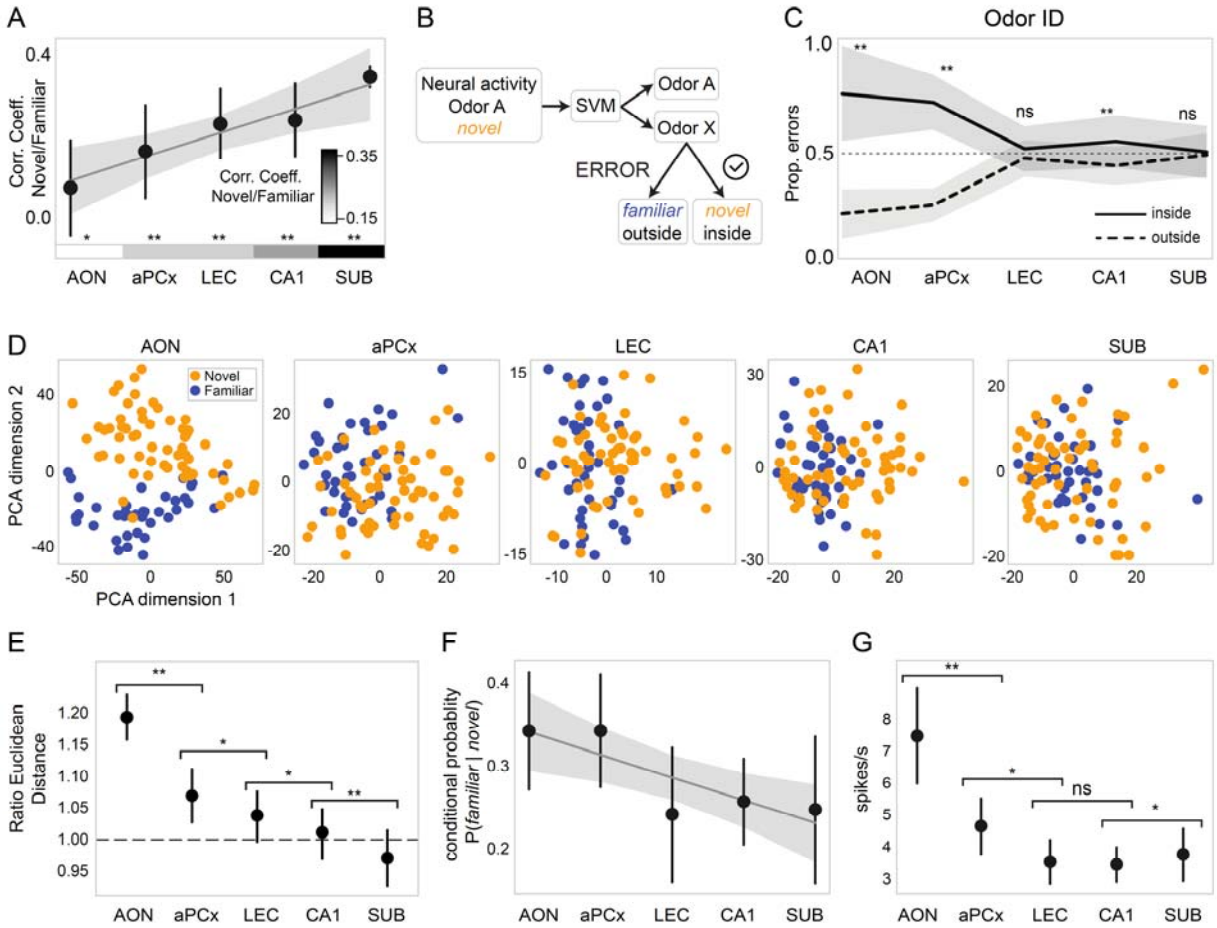

Figure 4. The representation of identity and experience become independent from each other along the cortico-hippocampal pathway. (A) Pearson correlation coefficients between SVM weights for decoding familiar and novel odor identity ($^{*}p<0.01$, $^{**}p<0.01$). Error bars: Standard error of the mean (SEM). **(B)** Schematic representation of the methodology to calculate error rate inside and outside the experience category (novel vs. familiar) with the example of a novel odor A. **(C)** Proportion of errors per region. Solid and dashed lines represent the proportion of errors inside and outside the same experience category, respectively. (*ns*: not significant, $^{**}p<0.01$, Wilcoxon rank-sum test). Error bars: SD. **(D)** Position of odors in the neural space for the 10 trials of four familiar odors (blue) and six novels (orange). The first two components of the PCA were used. Percentage explained by the first two dimensions: AON 31%, aPCx 15%, LEC 12%, CA1 15%, and SUB 28%. **(E)** Normalized Euclidean distance of principal components between novel and familiar odors divided by the average distance between all trials, pooled irrespective of experience ($p<0.01$, Kruskal-Wallis). Post-hoc pairwise comparison revealed significant differences between all regions ($^{*}p<0.05$, $^{**}p<0.01$, Mann-Whitney). Error bars: 95% CI of the mean. **(F)** Probability of responding to one or more familiar odors if a neuron responded to at least one novel odor ($p<0.001$, Kruskal-Wallis). AON and aPCx significantly different from LEC, CA1, and SUB ($p<0.01$, Mann-Whitney). Error bars: 95% CI of the mean. **(G)** Standard deviation of the firing rate in response to olfactory stimuli ($p<0.001$, Kruskal Wallis test). Response variability gradually decreases from AON to SUB (*ns*: not significant, $^{*}p<0.01$, $^{**}p<0.01$, Mann-Whitney). Error bars: 95% CI of the mean.

DISCUSSION

In this study we carried out extracellular recordings in awake, head-restrained mice performing a non-associative olfactory learning paradigm to characterize the transformation of olfactory representations from cortical primary sensory to multisensory areas in the medial temporal lobe. We analyzed neural responses to different novel and familiar olfactory stimuli in the AON, aPCx, LEC, CA1, and SUB to determine how odorant identity and odorant experience were reflected in each brain area. We found that both odor identity and olfactory experience were represented in every region, but representations were transformed between

brain areas along the pathway. In the AON, neurons were broadly tuned to different chemicals, and their responses were modulated by experience such that novel stimuli caused larger increases in firing rates than familiar stimuli. From the AON to hippocampal structures, the selectivity of neurons for specific odorants gradually increased, concurrent with the development of population-level odor representations, which became independent of novelty and familiarity. Consistent with this, we observed the emergence of specific populations of neurons tuned to select familiar odorants in aPCx and novel odorants in medial temporal lobe structures. These results suggest a gradual separation of the representations for identity and experience from AON to SUB.

The very first cortical processing stage, the AON, consistently outperformed all other brain areas in decoding accuracy for both stimulus features. Although the AON is the earliest cortical brain region involved in olfaction, it has thus far received remarkably little attention. This is in part because past research has focused on the aPCx, which is widely believed to carry the information for determining odorant identity (Bolding and Franks, 2017; Kadohisa and Wilson, 2006; Miura et al., 2012; Stettler and Axel, 2009). Our results are more consistent with an earlier hypothesis (Haberly, 2001) and recent experimental findings which suggest the AON plays a critical role in novel odor recognition(Rabell et al., 2017) and odor identification in general (Chae et al., 2022; Quintela et al., 2020). Hence, we support the view that the AON rather than aPCx should be considered as the primary sensory cortex in olfaction, but more research is needed to validate this hypothesis.

In the aPCx, we found a small population of neurons, specifically tuned to familiar odorants which might support the identification of known stimuli in the face of representational drift (Schoonover et al., 2021). Small, specialized subpopulations, like the one we identified in the aPCx might well provide a stable representation, even when most other neurons are unstable. However, they are easily overlooked due to the current limitations of longitudinal tracking of neurons. Approaches for tracking neurons with large-scale recording techniques (Van Beest et al., 2023; Yuan et al., 2024) will be instrumental in clarifying this question.

The finding that the LEC, CA1, and SUB represent the identity of odorants after they have been familiarized by passive exposure over several days might be considered surprising since nondeclarative learning is commonly viewed to be independent of medial temporal lobe structures (Squire et al., 2021, 2004). However, a specific projection from the CA1 to the AON has recently been shown to be critical for spatiotemporal odor memory in a nondeclarative behavioral paradigm (Aqrabawi and Kim, 2020)This suggests that the representation of specific odorant chemicals we observed might underlie the formation of contextual odor memories in CA1 and other medial lobe structures.

The analysis of the representation of experience in the LEC, CA1, and SUB offers additional important insights. Novel stimuli activated more neurons than familiar stimuli in the LEC, CA1, and SUB, which is in line with earlier descriptions of novelty-related activity in the hippocampus (Rolls et al., 1993). However, we did not find evidence for an abstract representation of novelty by stimulus-invariant "*novelty*" neurons. Consistent with the fact that hippocampal lesions do not disrupt novelty detection (Aqrabawi and Kim, 2020; Honey et al., 1998), our results thus offer a new perspective on the widely accepted interpretation that the hippocampus conveys a novelty signal to other brain structures, which broadly enhances attention and memory (Lisman and Grace, 2005; Ranganath and Rainer, 2003). Of note, previous studies had limited temporal or cellular resolution (Bunzeck and Düzel, 2006; Zhu et al., 1995), often used few novel stimuli, and did not report on stimulus-invariance (Xiang and Brown, 1998). Rather than encoding abstract stimulus novelty, our data suggests that the highly stimulus-selective neurons in LEC, CA1, and SUB represent stimulus identity, but an attentional gating mechanism causes their preferential activation when stimuli are novel. Further research is required to validate this hypothesis and to clarify the stimulus-invariance of individual neurons in response to novel stimuli from other sensory modalities and complex, multimodal stimuli, such as novel environments.

How experience affects sensory cortical representations has thus far mainly been studied in the visual system. Compared to familiar stimuli, novel stimuli induce larger activation in the visual cortex (Garrett et al., 2020; Homann et al., 2022), which can be explained by plasticity mechanisms inherent to neocortical circuits (Aitken et al., 2024). We found the same effect of stimulus novelty on response magnitude in the

AON, which is remarkable, given the anatomical differences between the AON, a 2-layered archeocortical structure, and the 6-layered neocortex. Collectively, these results suggest an evolutionary conserved mechanism for novelty processing is implemented in circuits with diverging architectures.

In conclusion, we propose a model (Figure 5) in which olfactory cortical areas represent stimulus identity with broadly tuned neurons, whose response magnitude is modulated by experience. This representation is gradually transformed such that stimulus identity becomes encoded by narrowly tuned neurons and experience by the number of active neurons. Future research involving simultaneous recordings along the cortico-hippocampal pathway will provide further insights into the processing of novel and familiar olfactory stimuli. While technically more challenging, simultaneous recordings can help to establish the temporal order of activation of different brain areas in order to resolve how the intricate network of feedforward and feedback connections supports encoding of stimulus identity and experience. Moreover, further work is needed to address the question if our findings extend to declarative paradigms, such as operant novelty detection tasks.

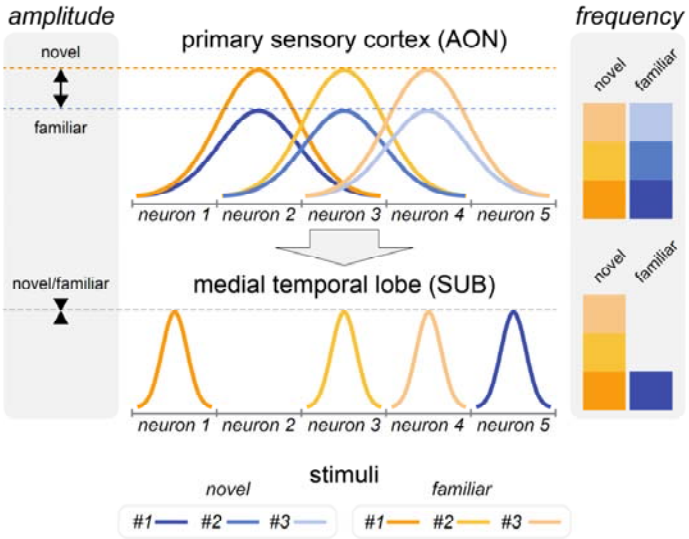

Figure 5. Proposed mechanism for the transformation of olfactory representations. Illustration showing the responses of 5 neurons in AON (top) and SUB (bottom) to either of 3 novel (orange) or familiar (blue) odorants. Novel stimuli evoked larger responses than familiar stimuli in the AON, whereas in hippocampal areas, novelty was reflected by the number of responsive neurons. Moreover, the stimulus selectivity decreases from AON to SUB (narrowing of response curves).

ACKNOWLEDGMENTS

This work was supported by Interne Fondsen KU Leuven C14/21/111 (SH), Fonds Wetenschappelijk Onderzoek-Vlaanderen (FWO-Flanders) fellowships 1135122N (ES) and 1272222N (CA), and grant G097022N (SH).

MATERIALS AND METHODS

Experimental model

Experiments were approved by KU Leuven Animal Ethics Committee under protocol P067/2017 and performed in accordance with the Federation of European Laboratory Animal Science Associations.

We used 13 male and 3 female mice between 18 and 30 weeks old, C57BL/6J (from KU Leuven). Animals were housed on a 12 h dark/12 h light cycle (dark from 07:00 to 19:00). Before the experiment, they were housed in groups of 2 to 4 mice until adult age, and at the start of the experiment, they were individually housed in GM500 cages (391 × 199 × 160 mm) with food and water *ad libitum*. Before starting behavioral tasks, animals were habituated to head-restrain for two days. All animals performed their task around the same time each day.

Surgical procedures

All mice were surgically implanted with a stainless-steel head plate to allow for head-restraining. Animals were anesthetized with ketamine and medetomidine mixture (60mg/Kg and 0.5mg/Kg of body weight intraperitoneally), and the depth of anesthesia was checked by monitoring tail pinch response, whisking and eye reflexes (as regularly throughout surgeries). If necessary, a booster shot of half the initial amount of anesthesia was given during the surgery. The head was shaved and then washed down with a series of Betadine (Meda, cat. no. 2990-257). The Xylocaine 5% (wt/wt) (Aspen, cat. no. 0137-398) was administered subcutaneously at a dose of 13 mg/Kg. Duratears (Alcon, cat. no. 0037-820) was applied to avoid dehydration of the eyes. Then mice were placed on a heating pad at 37°C (Harvard apparatus) in a stereotaxic frame (Narishige Instruments) using ear bars. An incision was made longitudinally along the top of the head, and a window of 2cm^2 was cut out to expose the underlying skull. Less than 50µL of Vet Bond (3M) was applied at the border between the skin and the skull to prevent irritation and scratching. A scalpel was used to remove connective tissue. The skull was dried using an air-blow device for 1 minute. The site of the craniotomy was then marked using a scalpel. Using a dental drill, ridges were created in the bone to increase the surface area of the skull for more adhesion. Dental cement (acrylic) was applied to glue the custom-made titanium head plate to the bone while leaving the site of the craniotomy free. The cement was let to dry for 10 minutes. The craniotomy was made in the shape of a circular hole of 1.5-2mm. A durotomy was made using a small precision scissor and a tweezer.

Subsequent steps following the craniotomy were performed according to whether recordings were conducted under acute or chronic conditions. For acute recordings, we used Neuropixels 1.0 probes (n=6); for chronic recordings, we used Neuropixels 2.0 probes (n=10). Before brain insertion, all probes were marked with a fluorescent dye (diI, Life Technologies). In animals designated for acute recordings, the craniotomy was covered with artificial dura to keep the exposed cortex healthy. Then, the craniotomy was closed with silicone (Kwik-Sil, World Precision Instruments). In animals designated for chronic recordings, probes were inserted using a micromanipulator at 200 µm/s per second to 600µm/s. Bone wax (Surgical Specialties, cat. No. 901) was applied over the probe insertion site to maintain a closed environment around the craniotomy site. Light curable dental cement (SDI Wave, cat. no. 7510203) was applied to secure the probe to the skull by curation with blue light.

At the end of each surgery, atipamezole (antisedan, 0.5mg/kg) was administered IP, immediately followed by the analgesic Metacam at 5-10 mg/kg. Animals were continually monitored until they regained consciousness.

Probes and coordinates

Type	Region	n=	Probe	AP (mm)	LM (mm)	Depth	Angle (°)
Acute	AON	3	1-shank	2.55-2.96	0.81-1.50	2.50-3.10	0-10 (latero-

							medial)
	aPCx	3	1-shank	1.00-2.34	1.25-1.95	2.75-4.00	
Chronic	AON	2*	4-shank	Shank 0: 2.90	0.80	3.00	
				Shank 1: 2.70			
				Shank 2: 2.50			
				Shank 3: 2.35			
	aPCx	4*	4-shank	Shank 0: 2.10-2.40	1.35-1.95	3.65-4.90	10 (anterior-posterior), 0-10 (latero-medial)
				Shank 1: 1.80-2.25			
				Shank 2: 1.70-2.10			
				Shank 3: 1.50-1.94			
	LEC & Hippocampus	5	4-shank	Shank 0: -3.535	2.75	4.50-5.00	15 (latero-medial)
				Shank 1: -3.285			
				Shank 2: -3.035			
				Shank 3: -2.785			

*one animal yielded units in both AON and aPCx.

Electrophysiological recordings

During acute recordings, the silicone seal covering the craniotomy was removed, and the probe was connected to the recording hardware and inserted using a micromanipulator. For chronic recordings, implanted probes were connected to the recording hardware. Setups were denoised with grounded metal structures attached to the recording system. Raw data was acquired using SpikeGLX software on a computer specifically dedicated to this use. Experimental events were acquired at 3 kHz by analog inputs on SpikeGLX. Respiration was monitored with a thermal camera (FLIR A325sc with 50μm lens, 60fps, 320×240 pixels) directed to the nostrils of the animal to capture respiration.

Odorants

The stimulus set consisted of 28 single-molecule substances (Sigma-Aldrich) commonly used in olfaction research. Odors were benzyl acetate, nonadienal, isoamyl acetate, heptanal, ethyldecanoate, linalyl formate, trimethylpyrazine, geraniol, geranyl acetate, salicylaldehyde, alpha-pheleandrene, thiophane, phenylethyl alcohol, dimethylpyrazine, limonene, carvone, octanoic acid, acetic acid, menthol, eugenol, benzaldehyde, ethyl methyl phenylglycidate, anisole, cinnamaldehyde, ethyl valerate and pentenoic acid. Each odor was dissolved in mineral oil to reach a final vapor pressure of 1Pa. Odors were delivered with a custom-made, constant air flow olfactometer, as described previously (Rabell et al., 2017).

Non-associative olfactory learning paradigm

All experiments were performed inside a sound and light isolated box (75*75*75 cm3) with constant exhaust to ensure rapid clearance of odorants. After recovery from the surgery (minimum 3 days), mice underwent habituation to head-restraining in the setup for one to three days. The paradigm was then performed essentially as described previously (Morrens et al., 2020). First, mice were familiarized with 4 odorants for 4 consecutive days. On subsequent days, novel odorants were introduced randomly interleaved with the previously familiarized odorants. All odors were delivered for 2 seconds and presented 10 times within one session. In recordings performed in AON and aPCx, a total of 8 novel odors were presented per session; in all other recording sessions, we used 6 novel odorants. To ensure that results were comparable between regions, we restricted our analysis to the first 6 novel stimuli presented. AON/aPCx recording sessions started with 4 presentations of familiar odorants, after which novel and familiar stimuli were presented in random order. In all other sessions, the order of odorant delivery was fully randomized. Two recording sessions were excluded from the analysis because 3 odorants which had been introduced as novel on the previous day, were mistakenly presented again.

Histology

Upon completion of experiments, mice received an overdose of ketamine/medetomidine, exsanguinated with PBS, and perfused with 4% paraformaldehyde. Brains were cut into 80μm coronal sections on a vibratome. Brain slices were mounted on glass slides using a VectaShield medium and analyzed using a confocal microscope to reconstruct anatomical recording locations based on the DiI label (Life Technologies), the probe's apparent trajectory, and the implantation's depth.

QUANTIFICATION AND STATISTICAL ANALYSIS

Processing of respiration signals

Videos recorded with the thermal camera were processed as described previously to extract inhalation onsets(Mutlu et al., 2018).

Preprocessing of the neural data

Electrophysiology data was preprocessed as described previously (Van Daal et al., 2021), using a combination of CatGT and kilosort 2.5. Following the automatic clustering, neurons were manually curated using phy2 to avoid multi-unit clusters, drifting neurons, or clusters with no refractory period.

auROC odor responses

We used the area under the receiver operating characteristic curve (auROC) to compute the change in firing rate during odor presentation. Spiking activity was first divided into 100ms bins. The baseline firing before odor delivery (the first 2s of each trial) was then compared with each bin afterward.

Responsiveness to odor and modulation by experience

Significant odorant responses were identified by comparing baseline firing rates before odorant delivery during the first 10 presentations of a given odor to the firing rate during the analysis window (Figure 2B) with a Wilcoxon rank test. A neuron was considered responsive to an odor if the test result was statistically significant. A similar approach was used to determine significant modulation by experience, performing the Wilcoxon rank test separately for novel and familiar stimuli. Neurons significant for both novel and familiar conditions were indicated as responding to both.

Gamma fit.

We used a methodology described previously (Maimon and Assad, 2009). In brief, the Inter-Spike Interval (ISI) of selected neurons was computed during the presentation of odors. The histogram distribution of the ISI was then fitted using a gamma function. Alpha parameters close to 1 signal a Poisson-like spiking dynamic.

Population decoding

Decoding was done using a linear Support Vector Machine (Kramer, 2016) to determine the identity of odorants (multi-class) or level of experience (binary class) using the firing rate of neurons in the analysis window (Figure 2B). Neurons from all sessions were concatenated. To allow for comparing the accuracy between regions, we subsampled the same number of neurons for each region (185 neurons). During 100 iterations, neurons were randomly chosen from the entire pool of neurons. Subsequently, neurons were divided into distinct sets for training and testing the SVM for each iteration. In order to mitigate the issue of overfitting, the Leave-1-out approach was used. Since sample sizes differed between regions, each iteration of the leave-one-out approach was averaged across different pools of decoded subpopulations. Thus, the variation (95%CI or SD) represents the fluctuation of performance of the SVM in trial-to-trial differences.

As there were more novel than familiar stimuli in our experimental paradigm, we took measures to balance the dataset for the SVM. For decoding experience, we used the first 40 trials of familiar and novel stimuli, respectively. For decoding odorant identity of novel and familiar stimuli separately, we used a Min-Max normalization (1) to balance different chance levels of decoding novel and familiar stimuli (Figure 3). (DA_{normed}: normalized decoding accuracy, Pc: chance level chance of the stimulus).

$$DA_{normed} = \frac{DA - Pc}{1 - Pc} \qquad (1)$$

Amplitude of the response

The difference in response amplitude to novel and familiar odors was computed for each neuron and was defined as the absolute value of the mean response to novel odor minus the mean response to familiar odor.

Mutual Information

Mutual information was calculated using the scikit learn library (Kramer, 2016) using a log base 2 (resulting in Shannon units – or bits). This allows for measuring the dependencies between two variables based on the methodologies described previously (Kraskov et al., 2004), which gives an entropy estimation from k-nearest neighbors distances (k=3). There is one discrete variable (odor identities) and one continuous (firing rate over consecutive trials). The function *mutual_info_classif* was used to quantify the amount of information recoverable on odor identities from the firing rate of cells. The mutual information was computed ten times for each cell-odor pair of one odor versus another odor (novel or familiar). This approach was repeated for the subpopulation analysis (Figure 3E).

Probability of responding to familiar odors

Fam_{Normed} and Nov_{Normed} refer to the normalized number of familiar and novel odors, respectively, to which a neuron significantly responded.

$$P(familiarity) = \frac{Fam_{Normed}}{Fam_{Normed}+Nov_{Normed}} \quad (2)$$

For each neuron responding to at least one novel odor, (2) was applied to obtain $P(familiarity|novelty)$

Grubbs test and novelty decoding

Using formula (2), $P(familiarity)$ and $P(novelty)$ were computed for each neuron responding to at least one novel or one familiar odor. A value of 1 for $P(novelty)$ indicates that the neuron is responding only to novel odor. A Grubb test was then used to evaluate whether those values indicated a particular outlier outside the normal range of the distribution.

Weight of the SVM

Weights of the SVM were extracted for the identity decoding of familiar and novel odors. The absolute value of those weights was used for the following analysis. The Pearson correlation for those weights was computed in Figure 4A. For the subpopulation analysis, neurons that had weights two times the standard deviation above the mean were counted (for familiar odors, AON=12, aPCx =11, LEC=13, SUB=8, CA1=24 and for novel odors, AON=15, aPCx =15, LEC=14, SUB=8, CA1=22) and used to compute the MI (Figure 3E).

Confusion matrix and proportion of errors inside/outside level of experience

The confusion matrix for the decoding of all odors was computed. The mean error inside the same category (novel odors are mistaken for other novel odors; familiar for other familiar odors) and outside the category (novel odors are mistaken for familiar odors; familiar for novel odors) were then assessed. The proportion of errors made inside or outside the category was then quantified. The variance reflects the variability between different test/training sets.

Distance in the neural space.

The spike rate of each neuron in the analysis window was extracted for the first ten presentations of familiar and novel odors. They were reduced into a 2D space using a PCA. The PCA space was normalized using a Min-Max method (3) per region and for each dimension. The distance between trials was evaluated using Euclidean distance in 2D. The inter-experience distance was measured between the familiar odor trials and the first six novel odors trials. The ratio of Figure 4G was computed by dividing the inter-experience distance by the inter-trials distance.

$$x_{normed} = \frac{x-x_{min}}{x_{max}-x_{min}} \quad (3)$$

REFERENCES

Aitken K, Campagnola L, Garrett ME, Olsen SR, Mihalas S. 2024. Simple synaptic modulations implement diverse novelty computations. *Cell Reports* **43**:114188. doi:10.1016/j.celrep.2024.114188

Aqrabawi AJ, Kim JC. 2020. Olfactory memory representations are stored in the anterior olfactory nucleus. *Nature Communications 2020 11:1* **11**:1–8. doi:10.1038/s41467-020-15032-2

Bathellier B, Buhl DL, Accolla R, Carleton A. 2008. Dynamic Ensemble Odor Coding in the Mammalian Olfactory Bulb: Sensory Information at Different Timescales. *Neuron* **57**:586–598. doi:10.1016/J.NEURON.2008.02.011

Bolding KA, Franks KM. 2018. Recurrent cortical circuits implement concentration-invariant odor coding. *Science* **361**. doi:10.1126/science.aat6904

Bolding KA, Franks KM. 2017. Complementary codes for odor identity and intensity in olfactory cortex. *eLife* **6**. doi:10.7554/ELIFE.22630

Bolding KA, Nagappan S, Han BX, Wang F, Franks KM. 2020. Recurrent circuitry is required to stabilize piriform cortex odor representations across brain states. *eLife* **9**:1–23. doi:10.7554/ELIFE.53125

Brady TF, Konkle T, Alvarez GA, Oliva A. 2008. Visual long-term memory has a massive storage capacity for object details. *Proceedings of the National Academy of Sciences* **105**:14325–14329. doi:10.1073/pnas.0803390105

Brunjes PC, Illig KR, Meyer EA. 2005. A field guide to the anterior olfactory nucleus (cortex). *Brain Research Reviews* **50**:305–335. doi:10.1016/j.brainresrev.2005.08.005

Bunzeck N, Düzel E. 2006. Absolute coding of stimulus novelty in the human substantia nigra/VTA. *Neuron* **51**:369–79. doi:10.1016/j.neuron.2006.06.021

Chae H, Banerjee A, Dussauze M, Albeanu DF. 2022. Long-range functional loops in the mouse olfactory system and their roles in computing odor identity. *Neuron* **110**:3970-3985.e7. doi:10.1016/j.neuron.2022.09.005

Cleland TA, Linster C. 2019. Central olfactory structures. pp. 79–96. doi:10.1016/B978-0-444-63855-7.00006-X

Craig S, Commins S. 2007. Plastic and metaplastic changes in the CA1 and subicular projections to the entorhinal cortex. *Brain Research* **1147**:124–139. doi:10.1016/j.brainres.2007.02.016

deCharms RC, Zador A. 2000. Neural Representation and the Cortical Code. *Annual Review of Neuroscience* **23**:613–647. doi:10.1146/annurev.neuro.23.1.613

Frenkel MY, Sawtell NB, Diogo ACM, Yoon B, Neve RL, Bear MF. 2006. Instructive Effect of Visual Experience in Mouse Visual Cortex. *Neuron* **51**:339–349. doi:10.1016/j.neuron.2006.06.026

Garrett M, Manavi S, Roll K, Ollerenshaw DR, Groblewski PA, Ponvert ND, Kiggins JT, Casal L, Mace K, Williford A, Leon A, Jia X, Ledochowitsch P, Buice MA, Wakeman W, Mihalas S, Olsen SR. 2020. Experience shapes activity dynamics and stimulus coding of VIP inhibitory cells. *eLife* **9**:e50340. doi:10.7554/eLife.50340

Haberly LB. 2001. Parallel-distributed Processing in Olfactory Cortex: New Insights from Morphological and Physiological Analysis of Neuronal Circuitry. *Chemical Senses* **26**:551–576. doi:10.1093/chemse/26.5.551

Haberly LB, Price JL. 1978. Association and commissural fiber systems of the olfactory cortex of the rat II. Systems originating in the olfactory peduncle. *Journal of Comparative Neurology* **181**:781–807. doi:10.1002/cne.901810407

Homann J, Koay SA, Chen KS, Tank DW, Berry MJ. 2022. Novel stimuli evoke excess activity in the mouse primary visual cortex. *Proceedings of the National Academy of Sciences of the United States of America* **119**:e2108882119. doi:10.1073/PNAS.2108882119/SUPPL_FILE/PNAS.2108882119.SM02.MP4

Honey RC, Watt A, Good M. 1998. Hippocampal lesions disrupt an associative mismatch process. *The Journal of neuroscience : the official journal of the Society for Neuroscience* **18**:2226–30. doi:10.1016/S0959-8049(09)70017-6

Kadohisa M, Wilson DA. 2006. Separate encoding of identity and similarity of complex familiar odors in piriform cortex. *Proceedings of the National Academy of Sciences* **103**:15206–15211. doi:10.1073/PNAS.0604313103

Kato HK, Chu MW, Isaacson JS, Komiyama T. 2012. Dynamic Sensory Representations in the Olfactory Bulb: Modulation by Wakefulness and Experience. *Neuron* **76**:962–975. doi:10.1016/J.NEURON.2012.09.037

Kramer O. 2016. Scikit-Learn. *Studies in Big Data* **20**:45–53. doi:10.1007/978-3-319-33383-0_5/FIGURES/2

Kraskov A, Stögbauer H, Grassberger P. 2004. Estimating mutual information. *Physical Review E - Statistical Physics, Plasmas, Fluids, and Related Interdisciplinary Topics* **69**:16. doi:10.1103/PHYSREVE.69.066138/FIGURES/20/MEDIUM

Kriegeskorte N, Wei X-X. 2021. Neural tuning and representational geometry. *Nature Reviews Neuroscience* **22**:703–718. doi:10.1038/s41583-021-00502-3

Leitner FC, Melzer S, Lütcke H, Pinna R, Seeburg PH, Helmchen F, Monyer H. 2016. Spatially segregated feedforward and feedback neurons support differential odor processing in the lateral entorhinal cortex. *Nature Neuroscience* **19**:935–944. doi:10.1038/nn.4303

Lisman JE, Grace AA. 2005. The hippocampal-VTA loop: controlling the entry of information into long-term memory. *Neuron* **46**:703–13. doi:10.1016/j.neuron.2005.05.002

Maimon G, Assad JA. 2009. Beyond Poisson: Increased Spike-Time Regularity across Primate Parietal Cortex. *Neuron* **62**:426–440. doi:10.1016/j.neuron.2009.03.021

Miura K, Mainen ZF, Uchida N. 2012. Odor Representations in Olfactory Cortex: Distributed Rate Coding and Decorrelated Population Activity. *Neuron* **74**:1087–1098. doi:10.1016/J.NEURON.2012.04.021

Morrens J, Rensburg AJV, Rabell JE, Haesler S. 2020. Cue-Evoked Dopamine Promotes Conditioned Responding during Learning. *Neuron* **106**:142-153.e7. doi:10.1016/j.neuron.2020.01.012

Mutlu K, Rabell JE, Olmo PM del, Haesler S. 2018. IR thermography-based monitoring of respiration phase without image segmentation. *Journal of Neuroscience Methods* **301**:1–8. doi:10.1016/J.JNEUMETH.2018.02.017

Neville KR, Haberly LB. 2003. Beta and Gamma Oscillations in the Olfactory System of the Urethane-Anesthetized Rat. *Journal of Neurophysiology* **90**:3921–3930. doi:10.1152/jn.00475.2003

Quintela RM, Bauer J, Wallhorn L, Le K, Brunert D, Rothermel M. 2020. Dynamic Impairment of Olfactory Behavior and Signaling Mediated by an Olfactory Corticofugal System. *The Journal of Neuroscience* **40**:7269–7285. doi:10.1523/JNEUROSCI.2667-19.2020

Rabell JE, Mutlu K, Noutel J, Olmo PM del, Haesler S. 2017. Spontaneous Rapid Odor Source Localization Behavior Requires Interhemispheric Communication. *Current Biology* **27**:1542-1548.e4. doi:10.1016/J.CUB.2017.04.027

Ranganath C, Rainer G. 2003. Neural mechanisms for detecting and remembering novel events. *Nature reviews Neuroscience* **4**:193–202. doi:10.1038/nrn1052

Rolls EdmundT, Cahusac PeterMB, Feigenbaum JanetD, Miyashita Y. 1993. Responses of single neurons in the hippocampus of the macaque related to recognition memory. *Exp Brain Res* **93**. doi:10.1007/BF00228398

Schoonover CE, Ohashi SN, Axel R, Fink AJP. 2021. Representational drift in primary olfactory cortex. *Nature* **594**:541–546. doi:10.1038/s41586-021-03628-7

Shin H, Moore CI. 2019. Persistent Gamma Spiking in SI Nonsensory Fast Spiking Cells Predicts Perceptual Success. *Neuron* **103**:1150-1163.e5. doi:10.1016/j.neuron.2019.06.014

Squire LR, Frascino JC, Rivera CS, Heyworth NC, He BJ. 2021. One-trial perceptual learning in the absence of conscious remembering and independent of the medial temporal lobe. *Proceedings of the National Academy of Sciences* **118**:e2104072118. doi:10.1073/pnas.2104072118

Squire LR, Stark CEL, Clark RE. 2004. The medial temporal lobe. *Annual Review of Neuroscience* **27**:279–306. doi:10.1146/annurev.neuro.27.070203.144130

Standing L. 1973. Learning 10000 pictures. *Quarterly Journal of Experimental Psychology* **25**:207–222. doi:10.1080/14640747308400340

Steinmetz NA, Aydin C, Lebedeva A, Okun M, Pachitariu M, Bauza M, Beau M, Bhagat J, Böhm C, Broux M, Chen S, Colonell J, Gardner RJ, Karsh B, Kloosterman F, Kostadinov D, Mora-Lopez C, O'Callaghan J, Park J, Putzeys J, Sauerbrei B, Van Daal RJJ, Vollan AZ, Wang S, Welkenhuysen M, Ye Z, Dudman JT, Dutta B, Hantman AW, Harris KD, Lee AK, Moser EI, O'Keefe J, Renart A, Svoboda K, Häusser M, Haesler S, Carandini M, Harris TD. 2021. Neuropixels 2.0: A miniaturized high-density probe for stable, long-term brain recordings. *Science* **372**:eabf4588. doi:10.1126/science.abf4588

Stettler DD, Axel R. 2009. Representations of Odor in the Piriform Cortex. *Neuron* **63**:854–864. doi:10.1016/j.neuron.2009.09.005

Su C-Y, Menuz K, Carlson JR. 2009. Olfactory Perception: Receptors, Cells, and Circuits. *Cell* **139**:45–59. doi:10.1016/j.cell.2009.09.015

Tsao A, Moser M-B, Moser EI. 2013. Traces of Experience in the Lateral Entorhinal Cortex. *Current Biology* **23**:399–405. doi:10.1016/j.cub.2013.01.036

Ulanovsky N, Las L, Nelken I. 2003. Processing of low-probability sounds by cortical neurons. *Nature Neuroscience* **6**:391–398. doi:10.1038/nn1032

Van Beest EH, Bimbard C, Fabre JMJ, Takács F, Coen P, Lebedeva A, Harris K, Carandini M. 2023. Tracking neurons across days with high-density probes. doi:10.1101/2023.10.12.562040

Van Daal RJJ, Aydin Ç, Michon F, Aarts AAA, Kraft M, Kloosterman F, Haesler S. 2021. Implantation of Neuropixels probes for chronic recording of neuronal activity in freely behaving mice and rats. *Nature Protocols* **16**:3322–3347. doi:10.1038/s41596-021-00539-9

Wesson DW, Carey RM, Verhagen JV, Wachowiak M. 2008. Rapid Encoding and Perception of Novel Odors in the Rat. *PLOS Biology* **6**:e82. doi:10.1371/JOURNAL.PBIO.0060082

Wilson DA. 1998. Habituation of Odor Responses in the Rat Anterior Piriform Cortex. *Journal of Neurophysiology* **79**:1425–1440. doi:10.1152/jn.1998.79.3.1425

Wilson DA, Stevenson RJ. 2003. The fundamental role of memory in olfactory perception. *Trends in Neurosciences* **26**:243–247. doi:10.1016/S0166-2236(03)00076-6

Witter MP, Moser EI. 2006. Spatial representation and the architecture of the entorhinal cortex. *Trends in Neurosciences* **29**:671–678. doi:10.1016/j.tins.2006.10.003

Witter MP, Naber PA, Haeften T van, Machielsen WC, Rombouts SA, Barkhof F, Scheltens P, Silva FHL da. 2000. Cortico-hippocampal communication by way of parallel parahippocampal-subicular pathways. *Hippocampus* **10**:398–410. doi:10.1002/1098-1063(2000)10:4<398::AID-HIPO6>3.0.CO;2-K

Woloszyn L, Sheinberg DL. 2012. Effects of Long-Term Visual Experience on Responses of Distinct Classes of Single Units in Inferior Temporal Cortex. *Neuron* **74**:193–205. doi:10.1016/j.neuron.2012.01.032

Wu T, Li S, Du D, Li R, Liu P, Yin Z, Zhang H, Qiao Y, Li A. 2023. Olfactory–auditory sensory integration in the lateral entorhinal cortex. *Progress in Neurobiology* **221**:102399. doi:10.1016/j.pneurobio.2022.102399

Xiang JZ, Brown MW. 1998. Differential neuronal encoding of novelty, familiarity and recency in regions of the anterior temporal lobeNeuropharmacology. pp. 657–676. doi:10.1016/S0028-3908(98)00030-6

Yuan A, Colonell J, Lebedeva A, Okun M, Charles AS, Harris TD. 2024. Multi-day Neuron Tracking in High Density Electrophysiology Recordings using EMD. doi:10.7554/eLife.92495.2

Zhu XO, Brown MW, McCabe BJ, Aggleton JP. 1995. Effects of the novelty or familiarity of visual stimuli on the expression of the immediate early gene c-fos in rat brain. *Neuroscience* **69**:821–829. doi:10.1016/0306-4522(95)00320-I